University of Groningen

A nonalcoholic fatty liver disease cirrhosis model in gerbil

Li, Wei; Guan, Zheng; Brisset, Jean C.; Shi, Qiaojuan; Lou, Qi; Ma, Yue; Suriguga, Su; Ying, Huazhong; Sa, Xiaoying; Chen, Zhenwen

IMPORTANT NOTE: You are advised to consult the publisher's version (publisher's PDF) if you wish to cite from it. Please check the document version below.

Document Version
Publisher's PDF, also known as Version of record

Publication date:
2018

[Link to publication in University of Groningen/UMCG research database](#)

Original Article
A nonalcoholic fatty liver disease cirrhosis model in gerbil: the dynamic relationship between hepatic lipid metabolism and cirrhosis

Wei Li[1,2], Zheng Guan[3], Jean C Brisset[6], Qiaojuan Shi[2], Qi Lou[2], Yue Ma[2], Su Suriguga[4], Huazhong Ying[2], Xiaoying Sa[2], Zhenwen Chen[5], Wim J Quax[3], Xiaofeng Chu[2]

[1]Laboratory Animal Center, Zhejiang University, Hangzhou, Zhejiang, China; [2]Laboratory Animal Center, Zhejiang Academy of Medical Sciences, Hangzhou, Zhejiang, China; Departments of [3]Chemical and Pharmaceutical Biology, [4]Pharmaceutical Technology and Biopharmacy, GUIDE, University of Groningen, Groningen, The Netherlands; [5]Department of Laboratory Animal Science, School of Basic Medical Science, Capital Medical University, Beijing, China; [6]Department of Radiology, New York University, New York, State of New York, The United States

Abstract: Nonalcoholic fatty liver disease (NAFLD) usually takes decades to develop into cirrhosis, which limits the longitudinal study of NAFLD. This work aims at developing a NAFLD-caused cirrhosis model in gerbil and examining the dynamic relationship between hepatic lipid metabolism and cirrhosis. We fed gerbil a high-fat and high-cholesterol diet (HFHCD) for 24 weeks, and recorded the gerbil's phenotype at 3, 6, 9, 12, 15, 18, 21, 24 weeks. The model's pathological process, lipid metabolism, oxidative stress, liver collagen deposition and presence of relevant cytokines were tested and evaluated during the full-time frame of disease onset. The gerbil model can induce nonalcoholic steatohepatitis (NASH) within 9 weeks, and can develop cirrhosis after 21 weeks induction. The model's lipids metabolism disorder is accompanied with the liver damage development. During the NAFLD progression, triglycerides (TG) and free fatty acids (FFA) have presented distinct rise and fall tendency, and the turning points are at the fibrosis stage. Besides that, the ratios of total cholesterol (CHO) to high-density lipoprotein cholesterol (HDL-C) exhibited constant growth tendency, and have a good linear relationship with hepatic stellate cells (HSC) (R^2 = 0.802, P < 0.001). The gerbil NAFLD cirrhosis model has been developed and possesses positive correlation between lipids metabolism and cirrhosis. The compelling rise and fall tendency of TG and FFA indicated that the fibrosis progression can lead to impairment in lipoprotein synthesis and engender decreased TG level. CHO/HDL-C ratios can imply the fibrosis progress and be used as a blood indicator for disease prediction and prevention.

Keywords: Cirrhosis, fibrosis, hepatic lipid metabolism, nonalcoholic fatty liver disease (NAFLD), gerbil

Introduction

Cirrhosis is a severe stage of liver dysfunction and is most commonly caused by alcohol, viral hepatitis, and NAFLD. Since NAFLD has become a leading health problem worldwide, especially for those people who are living with obesity [1], the lack of a suitable animal model for NAFLD-caused cirrhosis has aroused more and more attention. It has been suggested that 20% of the adult population in the world now has NAFLD [2], with an increase of 90% morbidity in obese populations [3]. The whole natural history of NAFLD has four stages: simple steatosis, NASH, fibrosis and cirrhosis. Fibrosis can lead to an increased morbidity rate from cirrhosis, hepatic failure, metabolic syndrome associated cardiovascular and cerebrovascular diseases, and hepatic carcinoma [4]. The clinical progression from simple steatosis to cirrhosis of NAFLD usually takes decades, strongly impacting the NAFLD-caused cirrhosis mechanism research and related drug development. For this reason, finding a suitable animal model for NAFLD-caused cirrhosis study becomes crucial.

Currently, NAFLD animal models can be divided into two types, one is the genetic model, and the other one is a drug and/or diet-induced

model. Most commonly used genetic models are related to lipid metabolism genes, such as ob/ob mouse, db/db mouse, (fa/fa) Zucker rats, PPARα-/- mouse, and PNPLA3 transgenic mouse. Whereas, spontaneous mutations are very rare in the clinic, and normally those cases are based on multiple gene mutations, which causes differences between clinic and the genetic models. For those drug and/or diet-induced models, the typical diets used to induce NAFLD are methionine choline deficient (MCD) diet [5, 6], high-fat diet (HFD, including high-fat and high-fat, high-cholesterol diets), and high-carbohydrate diet (HCD) [7]. Compared with the diet of human the MCD diet is abnormal, but HFD and HCD are similar. Additionally, comparing with the other animal models, our literature searches show that the rat HFD model is the more widely used model to investigate the etiology and pathogenesis of NAFLD [8-10]. However, this type of model cannot induce cirrhosis [11, 12]. The induced animal can reach NASH stage and fibrosis stage, but the fibrosis is mild and unstable. So in the past decade, a great emphasis has been placed on the animal models for NAFLD study.

The Mongolian gerbil (*Merionesunguiculatus*) is a fat-sensitive animal [13-18]. Its plasma lipid response to dietary fatty acids is more sensitive than humans, even without dietary cholesterol [13-18]. Due to its reported lipemic responses to dietary fat and cholesterol [13-20], the gerbil has been chosen to establish NAFLD animal model. Moreover, previous research findings have pointed out that NASH is associated with metabolic syndrome [21-25], and gerbil has the tendency to acquire diabetes spontaneously [26]. We attempt to establish a stable animal model, which shares the major clinical pathogenic factors: HFD, male, and lipid metabolism disorder [2]. Since we have clearly observed fibrosis stage and verified the stability of a gerbil NASH model in our former work [27, 28], the gerbil NASH model was used for developing a NAFLD-caused cirrhosis model and studying the mechanism. This is the first study to undertake a longitudinal observation of the whole natural history of NAFLD in gerbil and to investigate the dynamic relationship between hepatic lipid metabolism and cirrhosis. This is also the first comprehensive description of the new established NAFLD-

caused cirrhosis model. The model's pathological process, lipid metabolism, oxidative stress, liver collagen deposition and related cytokines were examined and evaluated in this research.

Methods

Animals

A total of 72 male littermate Mongolian gerbils (*Merionesunguiculatus*) were obtained from Zhejiang Academy of Medical Sciences, Zhejiang Center of Laboratory Animals (Hangzhou, China). All experiments were performed in accordance to the guidelines for animal care and use of Zhejiang province and Zhejiang Academy of Medical Sciences, and approved by the Ethics Committee of Zhejiang Academy of Medical Sciences (No. SCXK (Zhe) 2008-0033, and No. SYXK (Zhe) 2008-0113).

HFHCD for induction of NAFLD and cirrhosis

Gerbils were divided randomly into nine groups: one control group (n = 8) and eight time point model groups (each group, n = 8). The control group animals were fed a normal diet for 24 weeks, while the model group animals were fed an HFHCD. Based on former reports [29], we developed a new diet recipe (China Patent No. CN 102106476 A) to establish the model, which is similar to the western diet and containing the following components: 10% egg yolk powder (Zhejiang Changxing Ags Biological Products Co., Ltd.), 7% lard oil (purchased from local supermarket), 2.5% cholesterol (Huadong Pharmaceutical Co., Ltd) and 0.2% cholate (Huadong Pharmaceutical Co., Ltd). The nutritional differences of the diets are shown in Supplementary Table 1.

Experimental design

Every eight model animals were sacrificed at the end of week 3, 6, 9, 12, 15, 18, 21 and 24 for dynamic pathological and mechanical studies. Eight control animals were spared at the end of week 24. Blood samples were collected from abdominal aorta [30], allowed to clot for 2 hours at room temperature, centrifuged (3,500 × g, 10 min), and the supernatant was used for measurement of alanine transaminase (ALT), aspartate transaminase (AST), CHO, TG, HDL-C, low density lipoprotein choles-

terol (LDL-C) and glucose (GLU). Liver samples were obtained from the central part of the largest liver lobe. Liver homogenate was prepared to determine the content of FFA; and the following fibrosis indexes: type I collagen, type III collagen, transforming growth factor $\beta1$ (TGF-$\beta1$), and platelet-derived growth factor (PDGF), which were examined by western blotting (see Supplementary). Another part of the liver sample was fixed by 10% formalin and embedded in paraffin for histological study, and then were stained with hematoxylin and eosin (HE) and with Masson trichrome (for collagen). Besides, liver biopsy specimens were also immunohistochemically examined for Kupffer cells by assessing the expression of the receptor CD68, and HSC by evaluating the activation of the marker of HSC: alpha-smooth muscle actin (αSMA). As a double check, type I collagen and type III collagen were appraised as well as Kupffer cells and HSC by immunohistochemical examination. Meanwhile, for lipid accumulation assessment, electron microscope was employed to observe the liver tissue.

Biochemical analysis

The levels of serum ALT, AST, CHO, TG, GLU, LDL-C, and HDL-C were determined by an automatic chemical analyzer (HITACHI 7100, Japan). Commercial kits (Huifeng Science & Technology Co. Ltd., Shanghai, China; Jiancheng Biotech. Sci. Inc., Nanjing, China) were used for these analysis. All the procedures were followed as those stated in the protocols of the detection kits. Likewise, the levels of FFA in liver were examined by a Nonesterified free fatty acids assay kit (Jiancheng Biotech. Sci. Inc., Nanjing, China).

Histopathology, electron microscope observation and immunohistochemical analysis

For histopathological study, the liver sections were stained with HE and with Masson's trichrome. Histological steatosis, inflammation, and fibrosis were assessed semiquantitatively by a single-blinded pathologist, according to the scoring system proposed by Kleiner et al. [31]. During the assessment, a Leica microscope (Leica DM2500, Germany) was used for the observation. In each liver section, images of 10 random fields were taken (10 × 2.5 origi-

nal magnification; 0.22 mm^2 total area per image) for the judgment.

For transmission electron microscope observation, one animal was selected randomly from each group. After the liver was washed by using 0.9% physiological saline, a piece of the hepatic tissue was cut off from the central part of the largest liver lobe (about 1 × 1 × 1 mm). And then, the tissue was fixed in 2.5% glutaraldehyde for 4 hours at 4°C. Later, the samples were sent to electron microscopic laboratory (Virus Research Institute, Chinese Academy of Sciences), to gain the transmission electron microscope result.

The Kupffer cell, hepatic stellate cell, type I collagen, and type III collagen were detected using the common immunohistochemical method (see Supplementary). In order to show the fibrosis progression during the HFHCD induction clearly, an improved German immunohistochemical scoring (GIS) system [32] was employed to access the immunohistochemical slices. The percentage of positive cells was graded as follows: 0, negative; 1, up to 10% positive cells; 2, 11% to 20%; 3, 21% to 30%; 4, 31% to 40%; 5, 41% to 50%; 6, 51% to 60%; 7, 61% to 70%; 8, 71% to 80%; and 9, > 80%. The intensity of marker expression was graded as follows: 0, negative; 1, weakly positive; 2, moderately positive; 3, strongly positive. The final immunoreactive score equals to the product of the percentage of positive cells multiply the highest staining intensity.

Statistical analysis

Data are presented as the mean ± SD and compared by analysis of variance after validation of homoscedasticity using Bartlett's chi-square test. Statistical comparisons were carried out using the SPSS Statistics 19 system (IBM Corporation, Armonk, New York, USA) and freely available R programming language (v 3.2.5). The R package "scatterplot3d", "lmtest", "psych", "ggm", "car", "psy", and "ggplot2" were used in this study. The data set distribution was closer to a normal distribution. Then, a two-sample, two-sided t-test was applied to determine the significance of the differences between model group and the corresponding control group. The acceptable level of statistical significance was set at $P < 0.05$.
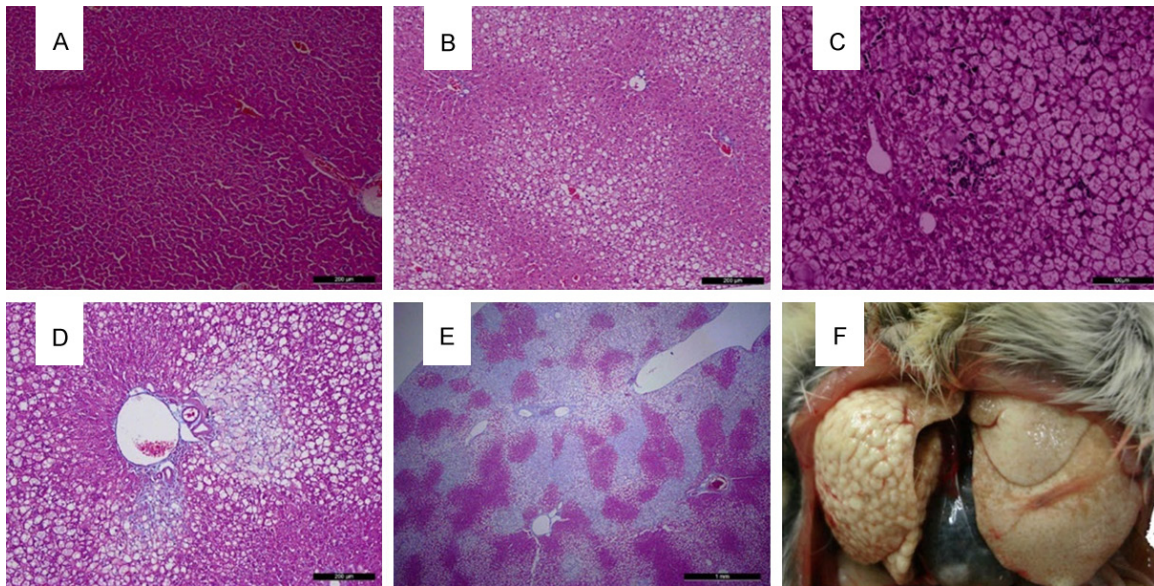
Figure 1. Hepatic injury of gerbil during the HFHCD treatment. A. Representative HE stained section of control liver. B. Representative HE section of the simple steatosis stage (6 weeks HFHCD treatment, gerbil liver). C. Representative HE section of NASH without fibrosis (12 weeks HFHCD treatment, gerbil liver). D. Representative HE section of NASH with fibrosis (18 weeks HFHCD treatment, gerbil liver). E. Representative HE section of cirrhosis stage (24 weeks HFHCD treatment, gerbil liver). F. Representative morphology picture of cirrhosis stage (24 weeks HFHCD treatment, gerbil liver).

Results

Histological and biochemical assessment of HFHCD induced NAFLD and cirrhosis

In the morphological observations, the control group gerbils have shown soft livers with normal color and smooth surfaces, whereas the model group gerbils presented different degrees of pathological liver over time. The liver of model group animals became swollen and hard and turned pale yellow, the edge of the pathological liver developed into a blunt shape, and the liver surface changed into an irregular pattern with whitish micronodules and macronodules (**Figure 1F**), which indicated the liver damage changes over the HFHCD induction time.

The comparison of histopathological study of the model group and control group has also shown a similar tendency as morphology observation. As exhibited in **Figure 1A**, no discernible histological alterations could be identified in control group. They had complete cytoplasm, sinusoidal spaces, distinct nucleus, nucleolus and central vein. In contrast, the model group presented a full blown cirrhosis feature accompanied with steatosis (**Figure 1E**),

and a significantly higher fibrosis score (Supplementary Table 2). These results provided microscopic evidence that indicated the significant liver damage changes over the HFHCD induction time. The independent pathological judgment [31] (Supplementary Table 2) show the obvious steatosis stage (**Figure 1B**) between 3 to 6 weeks, the NASH stage (**Figure 1C**, **1D**) between 9 to 18 weeks, and liver fibrosis stage (**Figure 1D**) after 12 weeks HFHCD induction. Finally, the cirrhosis model (**Figure 1E**, **1F**) can be seen to have been established after 21 weeks HFHCD induction (**Figure 2**).

Supplementary Tables 3 and 4 presented the results of raised ALT, AST, GLU, TG, CHO and body weight of model animals (0-9 weeks). These results exhibited the well repeated gerbil NASH model as we have reported before [27, 28].

In accord with the pathological assessment and transaminases results, in comparison to the control group, the immunohistochemical analysis and western blot results also show a compelling increase of type I ($P < 0.05$, after 21 weeks) and type III collagens ($P < 0.01$, after 15 weeks) in the model group (**Figure 3**). As shown in **Figure 3B**, After 15 weeks of HFHCD
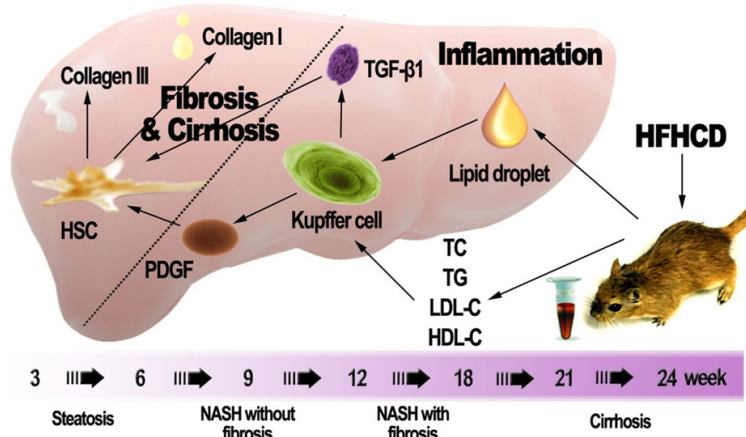
Figure 2. The four stages of the NAFLD-cirrhosis gerbil model and the tested indexes in this study.

induction, collagen III was increasing consistently ($P < 0.001$); on the other hand, collagen I was significantly increased again at week 24 ($P < 0.01$). Both of the type I and type III collagens reached the biochemical peak at week 24, which strengthen the assurance of the model.

Activation of Kupffer cell and HSC

Kupffer cells and hepatic stellate cells are generally regarded as keys of the fibrosis and cirrhosis mechanisms. In this study, Kupffer cells and hepatic stellate cells were evaluated by assessing the expression of the receptor CD-68, and αSMA, the marker of activated HSC. As expected, the control group animals only have few Kupffer cells, and no activated HSC has been observed (**Figure 3**). Whereas, the model groups show many Kupffer cells and HSC (**Figure 3**) after 12 weeks of HFHCD induction. Compare with the control group, the increase of Kupffer cells after 12 weeks HF-HCD induction is significant: 12 weeks, $P < 0.01$; 15 weeks, $P < 0.05$; 18 weeks, $P < 0.01$; 21 weeks, $P < 0.001$; and 24 weeks, $P < 0.01$. The comparison of the activated Kupffer cells between 18 weeks and 21 weeks model groups also shows compelling difference ($P < 0.05$). The HSC changes of model groups over the HFHCD induction time are significant too, as well as the tendency of Kupffer cells. HSC appeared together with the ballooning hepatocytes. Compared with the control group, the increase of HSC numbers after 12 weeks HF-HCD induction is notable: 12 weeks, $P < 0.01$; 15 weeks, $P < 0.01$; 18 weeks, $P < 0.001$; 21

weeks, $P < 0.001$; and 24 weeks, $P < 0.001$.

Hepatic expression of fibro-genesis mediators implicated in the fibrogenic process

Based on the western blot analysis, after 15 weeks HF-HCD induction, model group animals showed a significant protein expression increase of TGF-β1 and PDGF (**Figure 3C**), which are known to induce HSC activation and proliferation and also are responsible for the inflammation and vascular flow disarrangement. The correlation coefficient between the other variables and HSC measurements were calculated to be 0.68 for TGF-β1, 0.41 for PDGF and 0.62 for Kupffer cell (**Figure 4B**). The strong positive correlation between those chronic inflammation factors and HSC implies that the HFHCD induced cirrhosis may be partly caused by the chronic inflammation factors [11, 33], which directly induced the activation of HSC. Besides that, partial correlation analysis shows that TGF-β1 has a strong positivecorrelation with HSC, its partial correlation coefficient is 0.65, which is similar to their correlation coefficient mentionedabove (0.68, TGF-β1 and HSC). This result suggests that TGF-β1 and HSC has a strong and direct positive correlation. The followed-up statistical analysis also indicates TGF-β1 is prior to HSC and is the Granger-cause of HSC ($P < 0.05$, optimal lagorder is determined by Akaike information criteria) [34, 35]. Since TGF-β1 is the Granger-cause of HSC, along with HFHCD feeding time, we calculated their linear regression formula: HSC = 2.467 + 1.279e^{-5} × TGF-β1 + 1.831e^{-1} × Time (R^2 = 0.764, TGF-β1 is based on the gray scale values of western blotting result [36]) (**Figure 4B**), and their coefficients are significant ($P < 0.001$). Its good linear relation offers TGF-β1 as a new supplement indicator for fibrosis diagnosis and prediction.

Dynamic relationship between hepatic lipid metabolism and cirrhosis

The lipid accumulation in liver was observed by transmission electron microscopy. The ul-
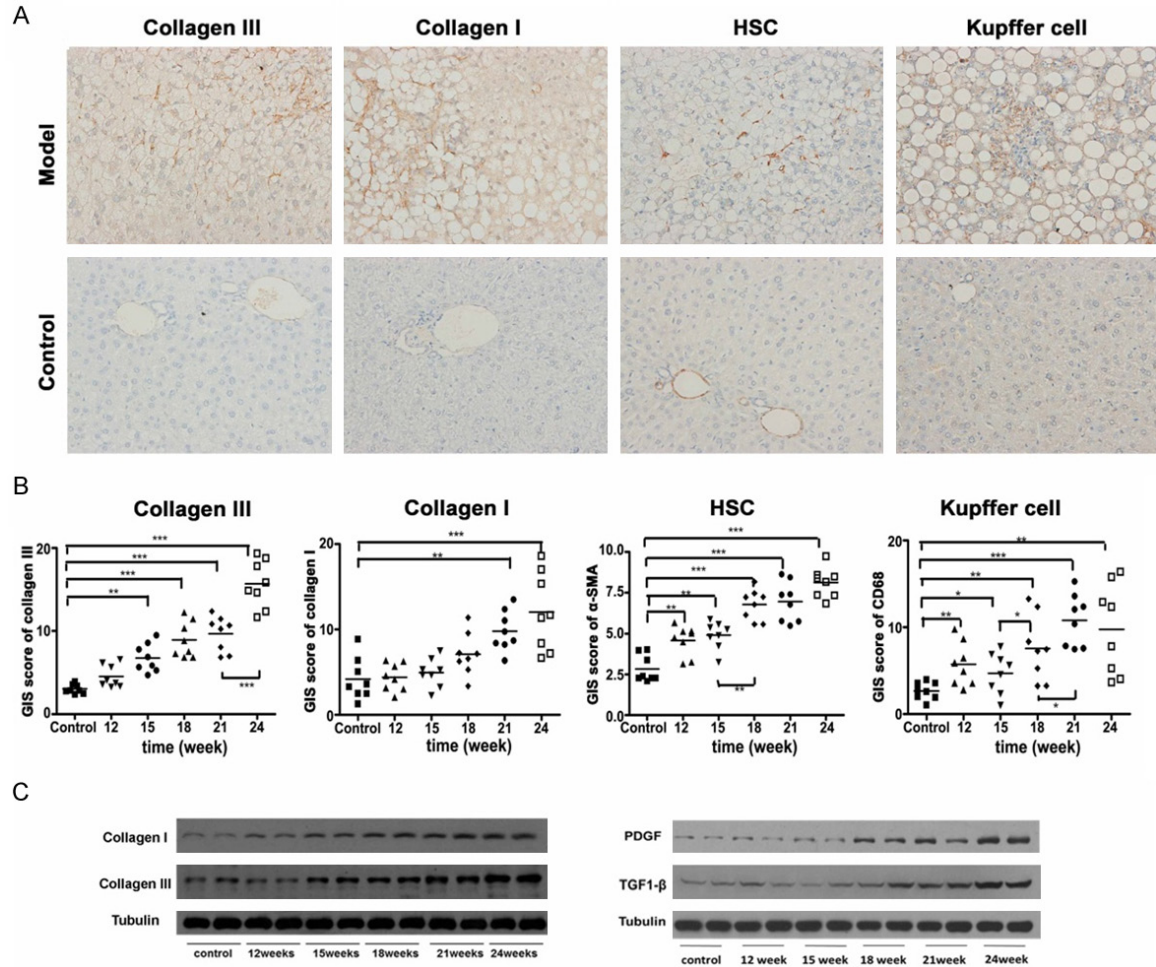
Figure 3. Hepatic fibrosis of gerbil during the HFHCD treatment. (A) Representative immunohistochemical sections (model groups: collagen III, 15 weeks HFHCD treatment; collagen I, 21 weeks HFHCD treatment; HSC, 21 weeks HFHCD treatment; Kupffer cell, 24 weeks HFHCD treatment) and (B) German immunohistochemical scoring (GIS) of collagen III, collagen I, αSMA, and CD68 of gerbil liver. (C) Western blot results of collagen III, collagen I, PDGF, and TGF-β1.*$P < 0.05$, **$P < 0.01$, ***$P < 0.001$.

trastructure of hepatic cells was normal in control group: the membrane was well defined; chromatin was uniformly distributed. No fat droplet could be found in mitochondria, endocytoplasmic reticulum or liver cell. The cell nucleus was overall in shape (**Figure 5A**). In contrast, the model group animals have many fat droplets and formation of vacuoles in liver cells. After 3 weeks HFHCD induction, the small lipid droplets appeared everywhere in the cell (**Figure 5B**, **5C**). And then, during the HFHCD induction process, the fat droplets accumulated into some big lipid droplets (**Figure 5E**, **5F**). The observed lipid accumulation changes indicated the severity degree of hepatic lipid metabolism disorder, which also complies with the NAFLD progression. In addition, total CHO, LDL-C, FFA and HDL-C were increased dramatically in relation to the HFHCD induction time (**Figures 5D** and **4A**). To illustrate the dynamic relationship between hepatic lipid metabolism and cirrhosis, a focused principal components analysis (FPCA) has been performed [37]. Since TG and FFA have shown distinct rise and fall tendency, and the turning point is at 18 weeks and 12 weeks (fibrosis stage). Accordingly, FPCA also reflected the differences. The analysis has shown significant positive correlation between HSC and all the tested factors (*P* < 0.05), except FFA and TG (**Figure 4B**). FPCA revealed that HDL-C, LDL-C, and CHO belong to the main factors in this experiment, and their increment can promote the fibrosis progression (**Figure 4B**).
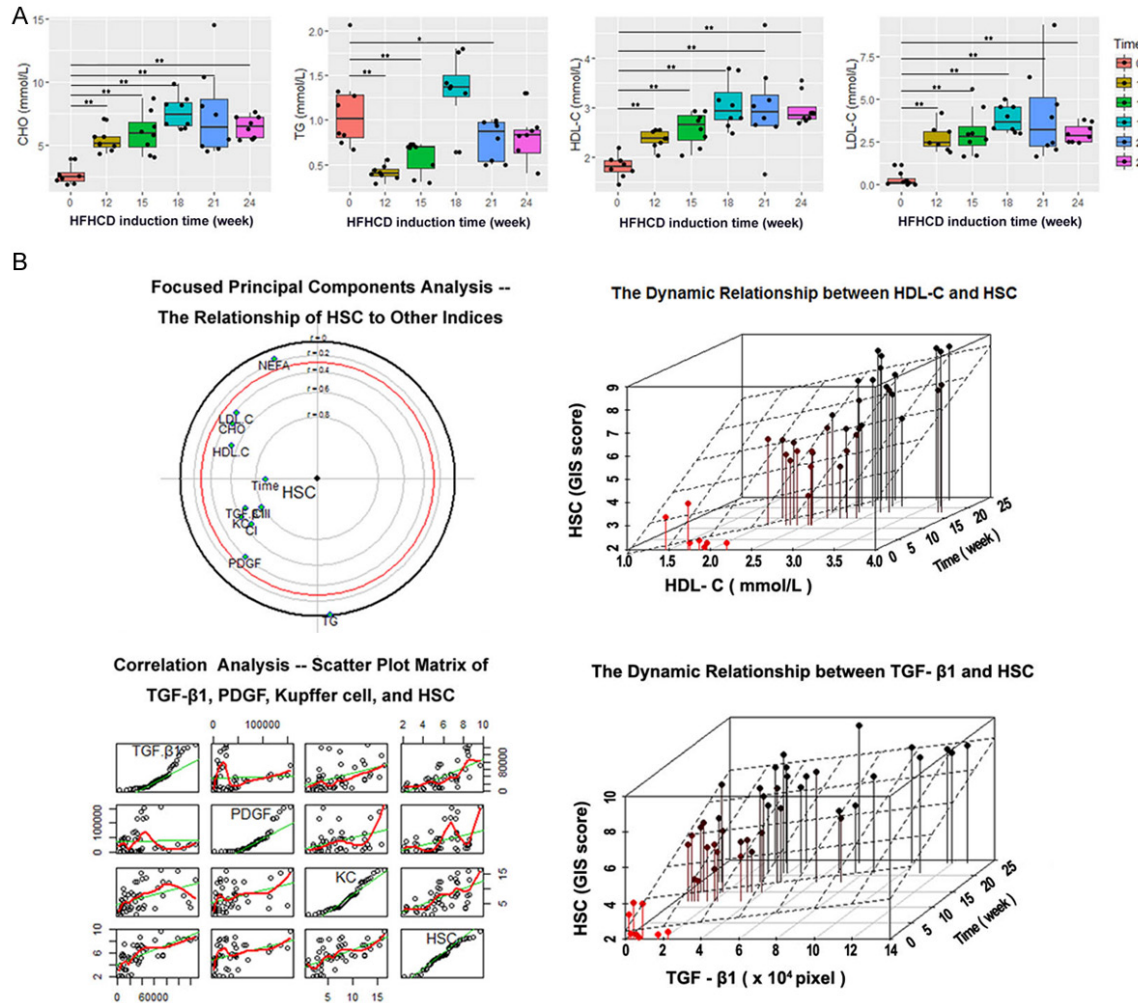
Figure 4. The dynamic relationship between gerbil hepatic lipid metabolism and fibrogenesis indicators and mediators. A. The blood lipids changes of gerbil during the HFHCD treatment. B. The positive correlation of gerbil HSC, CI, CIII, Kupffer cell, PDGF, TGF-β1, CHO, HDL-C, LDL-C, FFA and TG (P < 0.05, except FFA and TG); and two linear regression models. The dynamic relationship between HDL-C and HSC. The dynamic relationship between TGF-β1 and HSC (TGF-β1 is based on the gray scale values of western blotting result [36]). *P < 0.05, **P < 0.01.

Discussion

Our novel data shows that in the first 9 weeks HFHCD induction, the model's body weight, GLU, ALT, AST, CHO, and TG levels were significantly increased (Supplementary Tables 3 and 4). The histological scoring system also shows the NASH features. Therefore, the gerbil NASH model has been repeated well as our former studies [27, 28]. During the whole study period, a number of features in common with human disease were found: (i) the excessive accumulation of FFA, (ii) blood lipid metabolism disorder, (iii) cellular ballooning, (iv) immunohistochemistry changes, and (v) liver morphology modifications [38-40]. Progres-

sion of the cirrhosis from NAFLD was clearly subdivided into stages (**Figure 2**) allowing the study of the progression of the disease and the correlation with the HFHCD induction time. The result indicates a strong positive correlation between lipids metabolism and cirrhosis, which mimics the clinical disease. Therefore, the gerbil NAFLD cirrhosis model has been established and can be used to study NAFLD progression, especially the cirrhosis stage, for a better understanding of the disease pathophysiology and for medicine development.

Besides, during the longitudinal study we have observed a distinct rise and fall tendency of TG and FFA levels, and their turning points are
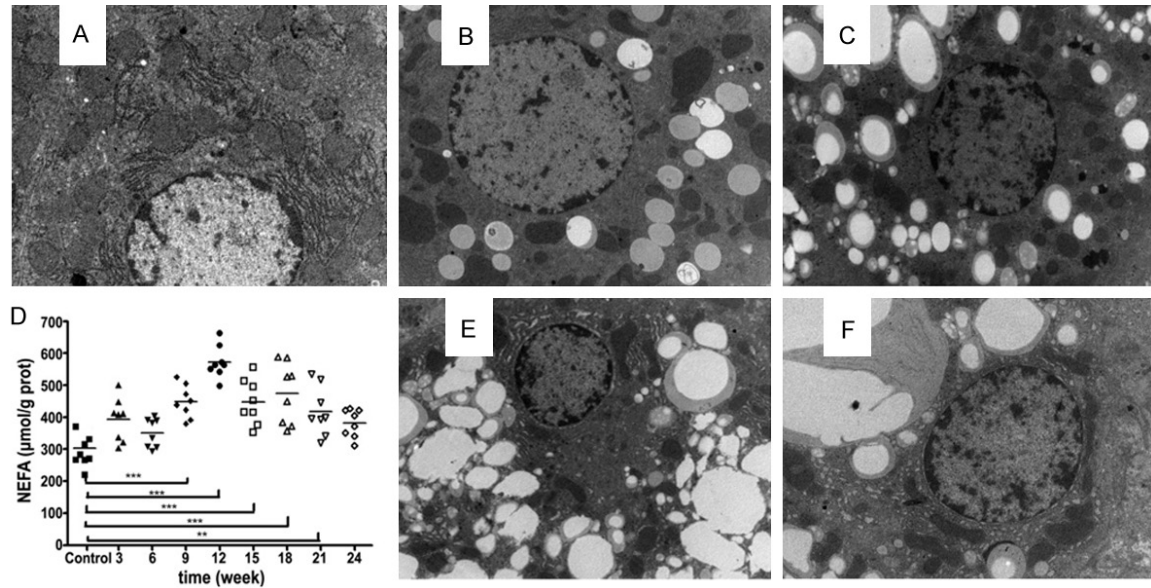
Figure 5. Hepatic lipid metabolism of gerbil during the HFHCD treatment. (light gray circular area is accumulated triglyceride and the dark gray circular area is cholesteryl ester). A. Representative transmission electron micrograph of control liver. B. Representative transmission electron micrograph of the fatty liver steatosis stage (3 weeks). C. Representative transmission electron micrograph of the NASH stage (9 weeks). E, F. Representative transmission electron micrograph of the fibrosis and cirrhosis stages (15 and 21 weeks). D. The FFA level changes in gerbil liver during the HFHCD treatment.**P < 0.01, ***P < 0.001.

in the fibrosis stage. The decreased TG level seems rare based on our knowledge. Coincidently, a Harvard group has also reported the similar tendency recently [41]. Their clinical study statistically analyzed 11947 cases, and pointed out that lower triglyceride levels may indicate more advanced liver disease. The fibrosis progression caused liver dysfunction can possibly lead to resultant impairment in lipoprotein synthesis and result in decreased triglyceride export. The accompanied FFA level changes are the support of the inference.

Since the gerbil NAFLD cirrhosis model has been well developed, which not only possess the similar clinical features but also can be clearly divided into stages, we tried FPCA to find out the closest indexes of HSC for the dynamic monitoring and disease progression prognosis. The FPCA [37] result indicated that HDL-C, LDL-C, and CHO are closely related with HSC and other fibrosis indicators in the NAFLD-cirrhosis progression. The similar increasing tendency of Kupffer cells, HSC, TGF-β1, and PDGF also supports previous research into this area which indicated that the Kupffer cells can secrete TGF-β1, and PDGF to stimulate fibrosis development through the mitogenic

stimuli of them on HSC [42]. Surprisingly, the growth of HDL-C was found abnormal during the HFHCD induction time, which has aroused our attention. In this study, HDL-C not only has strong positive correlation with HSC (r = 0.556, P < 0.05), but also has a good linear relationship with HSC along with the HFHCD induction time (**Figure 4B**, HSC = 1.047 + 0.756 × HDL-C + 0.178 × Time, R^2 = 0.823, P < 0.001). A few NAFLD studies [43, 44] have also reported the same HDL-C increase tendency, which may suggest the special mechanism during the NAFLD-caused fibrosis progression. So we looked into the CHO/HDL-C ratio to further inspect the model. It is interesting to note that the CHO/HDL-C ratios show constant growth tendency during the HFHCD induction, and have good linear relationship with HSC (HSC = 3.542 - 0.655 × CHO/HDL-C + 0.237 × Time, R^2 = 0.802, P < 0.001). These results are dramatically consistent with the clinic reports [45, 46] and may imply the special status of HDL-C in the NAFLD progression. Considering the possible HFD or HFHCD differences, environment differences, and animal differences in other labs, we suggest using CHO/HDL-C ratio as a convenient blood indicator for the standard gerbil model assessment. For this

purpose, the blood sample can be collected from the tail vein or the cheek vein (300 μL blood is enough for detecting more than two indexes), and the regression equation might be used to determine the NAFLD stage and suitable experiment time.

As we presented in the result, the pros and cons of this gerbil NAFLD cirrhosis model can easily be listed. First of all, this gerbil model can induce NASH within 9 weeks, and can develop stable cirrhosis after 21 weeks HFH-CD induction (Supplementary Table 2). This is in contrast to, as Robert Schierwagen reported, most of the existing HFD induced NAFLD models that need a minimum of 15 weeks induction and that hardly show stable fibrosis [23, 47-49]. Secondly, the model has the same fibrosis progression (eg. HSC activation, collagen III and collagen I deposition, bridging fibrosis, and cirrhosis) as in the clinic [38-40], and leads to a stable cirrhosis stage. It can thus be suggested that the gerbil model can cover the whole NAFLD disease spectrum to make up the NAFLD model deficiency [11, 12]. Having the same features and etiologies as the clinical process combined with its stable cirrhosis stage, is key advantage of this gerbil model for the NAFLD and cirrhosis investigations. As still remaining limitations of the gerbil model we can mention that the additional diet cholesterol may cause some metabolism differences. Further studies are required to address whether alterations in diet composition can lead to a refined model, which can completely reproduce the human disease mechanism. Besides that, the 21 weeks cirrhosis induction time is still not very convenient. If the research purpose is only to study the cirrhosis stage, it would be meaningful to further improve the HFHCD recipe for the gerbil model.

In summary, we have firstly established a gerbil NAFLD cirrhosis model, which has stable fibrosis stage and can be used for NAFLD longitudinal study. The study shows for the first time that the lipids metabolism disorder is accompanied with liver damage during the whole NAFLD progression, and they have a positive correlation along with the HFHCD induction time. The dynamic observation also initially detected the noticeable rise and fall tendency of TG and FFA levels during the NAFLD progression. Moreover, the good linear relationship between CHO/HDL-C and HSC pioneered that the CHO/HDL-C ratio can be a convenient biomarker for the NAFLD progression judgment, especially for the fibrosis progression diagnosis and prediction.

Acknowledgements

Disclosure of conflict of interest

None.

Address correspondence to: Dr. Zhenwen Chen, Department of Laboratory Animal Science, School of Basic Medical Science, Capital Medical University, Beijing 100069, China. Tel: +86 10 83911495; E-mail: czwen@ccmu.edu.cn; Dr. Wim J Quax, Department of Chemical and Pharmaceutical Biology, GUIDE, University of Groningen, Groningen, 9713 AV, The Netherlands. Tel: +31 503632558; Fax: +31 503633000; E-mail: w.j.quax@rug.nl; Dr. Xiaofeng Chu, Laboratory Animal Center, Zhejiang Academy of Medical Sciences, Hangzhou 310013, Zhejiang, China. Tel: +86 571 86952350; Fax: +86 571 88208070; E-mail: sydw@zjinfo.gov.cn

References

[1] Henao-Mejia J, Elinav E, Jin C, Hao L, Mehal WZ, Strowig T, Thaiss CA, Kau AL, Eisenbarth SC, Jurczak MJ, Camporez JP, Shulman GI, Gordon JI, Hoffman HM and Flavell RA. Inflammasome-mediated dysbiosis regulates progression of NAFLD and obesity. Nature 2012; 482: 179-185.

[2] Chalasani N, Younossi Z, Lavine JE, Diehl AM, Brunt EM, Cusi K, Charlton M and Sanyal AJ. The diagnosis and management of non-alcoholic fatty liver disease: practice guideline by the American association for the study of liver diseases, American college of gastroenterology, and the American gastroenterological association. Hepatology 2012; 55: 2005-2023.

[3] Torres DM and Harrison SA. Diagnosis and therapy of nonalcoholic steatohepatitis. Gastroenterology 2008; 134: 1682-1698.

[4] Younossi ZM, Otgonsuren M, Henry L, Venkatesan C, Mishra A, Erario M and Hunt S. Association of nonalcoholic fatty liver disease (NAFLD) with hepatocellular carcinoma (HCC) in the United States from 2004 to 2009. Hepatology 2015; 62: 1723-1730.

[5] Chae MK, Park SG, Song SO, Kang ES, Cha BS, Lee HC and Lee BW. Pentoxifylline attenuates methionine- and choline-deficient-diet-induced steatohepatitis by suppressing TNF-alpha expression and endoplasmic reticulum stress. Exp Diabetes Res 2012; 2012: 762565.

[6] Loyer X, Paradis V, Hénique C, Vion AC, Colnot N, Guerin CL, Devue C, On S, Scetbun J, Romain M, Paul JL, Rothenberg ME, Marcellin P, Durand F, Bedossa P, Prip-Buus C, Baugé E, Staels B, Boulanger CM, Tedgui A, Rautou PE. Liver microRNA-21 is overexpressed in non-alcoholic steatohepatitis and contributes to the disease in experimental models by inhibiting PPARα expression. Gut 2015; 65: 1882-1894.

[7] Feldstein AE, Canbay A, Guicciardi ME, Higuchi H, Bronk SF and Gores GJ. Diet associated hepatic steatosis sensitizes to Fas mediated liver injury in mice. J Hepatol 2003; 39: 978-983.

[8] Pasarin M, Abraldes JG, Rodriguez-Vilarrupla A, La Mura V, Garcia-Pagan JC and Bosch J. Insulin resistance and liver microcirculation in a rat model of early NAFLD. J Hepatol 2011; 55: 1095-1102.

[9] Thomsen KL, Gronbaek H, Glavind E, Hebbard L, Jessen N, Clouston A, George J and Vilstrup H. Experimental nonalcoholic steatohepatitis compromises ureagenesis, an essential hepatic metabolic function. Am J Physiol Gastrointest Liver Physiol 2014; 307: G295-301.

[10] Thomsen KL, Hebbard L, Glavind E, Clouston A, Vilstrup H, George J and Gronbaek H. Nonalcoholic steatohepatitis weakens the acute phase response to endotoxin in rats. Liver Int 2014; 34: 1584-1592.

[11] Kucera O and Cervinkova Z. Experimental models of non-alcoholic fatty liver disease in rats. World J Gastroenterol 2014; 20: 8364-8376.

[12] Hebbard L and George J. Animal models of nonalcoholic fatty liver disease. Nat Rev Gastroenterol Hepatol 2011; 8: 35-44.

[13] Hegsted DM and Gallagher A. Dietary fat and cholesterol and serum cholesterol in the gerbil. J Lipid Res 1967; 8: 210-214.

[14] Mercer NJ and Holub BJ. Response of free and esterified plasma cholesterol levels in the Mongolian gerbil to the fatty acid composition of dietary lipid. Lipids 1979; 14: 1009-1014.

[15] Nicolosi RJ, Marlett JA, Morello AM, Flanagan SA and Hegsted DM. Influence of dietary unsaturated and saturated fat on the plasma lipoproteins of Mongolian gerbils. Atherosclerosis 1981; 38: 359-371.

[16] Andersen DB and Holub BJ. Effects of dietary cholesterol level and type of dietary carbohydrate on hepatic and plasma sterols in the gerbil. Can J Physiol Pharmacol 1982; 60: 885-892.

[17] Dictenberg JB, Pronczuk A and Hayes KC. Hyperlipidemic effects of trans fatty acids are accentuated by dietary cholesterol in gerbils. J Nutr Biochem 1995; 6: 353-361.

[18] Wijendran V, Pronczuk A, Bertoli C and Hayes KC. Dietary trans-18:1 raises plasma triglycerides and VLDL cholesterol when replacing either 16:0 or 18:0 in gerbils. J Nutr Biochem 2003; 14: 584-590.

[19] Forsythe WA 3rd. Comparison of dietary casein or soy protein effects on plasma lipids and hormone concentrations in the gerbil (Meriones unguiculatus). J Nutr 1986; 116: 1165-1171.

[20] Tracy E, Tasker and Potter SM. Effects of dietary protein source on plasma lipids, HMG CoA reductase activity, and hepatic glutathione levels in gerbils. J Nutr Biochem 1993; 4: 458-462.

[21] Marchesini G, Brizi M, Bianchi G, Tomassetti S, Bugianesi E, Lenzi M, McCullough AJ, Natale S, Forlani G and Melchionda N. Nonalcoholic fatty liver disease: a feature of the metabolic syndrome. Diabetes 2001; 50: 1844-1850.

[22] Sanyal AJ, Campbell-Sargent C, Mirshahi F, Rizzo WB, Contos MJ, Sterling RK, Luketic VA, Shiffman ML and Clore JN. Nonalcoholic steatohepatitis: association of insulin resistance and mitochondrial abnormalities. Gastroenterology 2001; 120: 1183-1192.

[23] Schierwagen R, Maybuchen L, Zimmer S, Hittatiya K, Back C, Klein S, Uschner FE, Reul W, Boor P, Nickenig G, Strassburg CP, Trautwein C, Plat J, Lutjohann D, Sauerbruch T, Tacke F and Trebicka J. Seven weeks of Western diet in apolipoprotein-E-deficient mice induce metabolic syndrome and non-alcoholic steatohepatitis with liver fibrosis. Sci Rep 2015; 5: 12931.

[24] Meex RC, Hoy AJ, Morris A, Brown RD, Lo JC, Burke M, Goode RJ, Kingwell BA, Kraakman MJ, Febbraio MA, Greve JW, Rensen SS, Molloy MP, Lancaster GI, Bruce CR and Watt MJ. Fetuin B is a secreted hepatocyte factor linking steatosis to impaired glucose metabolism. Cell Metab 2015; 22: 1078-1089.

[25] Pais R, Barritt AS 4th, Calmus Y, Scatton O, Runge T, Lebray P, Poynard T, Ratziu V and Conti F. NAFLD and liver transplantation: Current burden and expected challenges. J Hepatol 2016; 65: 1245-1257.

[26] Boquist L. Obesity and pancreatic islet hyperplasia in the Mongolian gerbil. Diabetologia 1972; 8: 274-282.

[27] Li W, Shi QJ, Guo HG, Lou Q, Lu LQ and Sa XY. Dynamic analysis of the pathogenesis and biochemistry of nonalcoholic fatty liver disease in gerbils. Chinese Journal of Laboratory Animal Science 2011; 21: 44-48.

[28] Ying HZ, Liu YH, Yu B, Wang ZY, Zang JN and Yu CH. Dietary quercetin ameliorates nonalcoholic steatohepatitis induced by a high-fat diet in gerbils. Food Chem Toxicol 2013; 52: 53-60.

[29] Ioannou GN, Morrow OB, Connole ML and Lee SP. Association between dietary nutrient composition and the incidence of cirrhosis or liver cancer in the United States population. Hepatology 2009; 50: 175-184.

[30] Panchal SK, Poudyal H, Arumugam TV and Brown L. Rutin attenuates metabolic changes, nonalcoholic steatohepatitis, and cardiovascular remodeling in high-carbohydrate, high-fat diet-fed rats. J Nutr 2011; 141: 1062-1069.

[31] Kleiner DE, Brunt EM, Van Natta M, Behling C, Contos MJ, Cummings OW, Ferrell LD, Liu YC, Torbenson MS, Unalp-Arida A, Yeh M, McCullough AJ and Sanyal AJ. Design and validation of a histological scoring system for nonalcoholic fatty liver disease. Hepatology 2005; 41: 1313-1321.

[32] Remmele W and Schicketanz KH. Immunohistochemical determination of estrogen and progesterone receptor content in human breast cancer. Computer-assisted image analysis (QIC score) vs. subjective grading (IRS). Pathol Res Pract 1993; 189: 862-866.

[33] Marra F, Gastaldelli A, Svegliati Baroni G, Tell G and Tiribelli C. Molecular basis and mechanisms of progression of non-alcoholic steatohepatitis. Trends Mol Med 2008; 14: 72-81.

[34] Zeileis A and Hothorn T. Diagnostic checking in regression relationships. R News 2002; 2: 7-10.

[35] Sherman KE, Guedj J, Shata MT, Blackard JT, Rouster SD, Castro M, Feinberg J, Sterling RK, Goodman Z, Aronow BJ and Perelson AS. Modulation of HCV replication after combination antiretroviral therapy in HCV/HIV co-infected patients. Sci Transl Med 2014; 6: 246ra298.

[36] Yang Q, Pan Q, Li C, Xu Y, Wen C and Sun F. NRAGE is involved in homologous recombination repair to resist the DNA-damaging chemotherapy and composes a ternary complex with RNF8-BARD1 to promote cell survival in squamous esophageal tumorigenesis. Cell Death Differ 2016; 23: 1406-1416.

[37] Bayen E, Pradat-Diehl P, Jourdan C, Ghout I, Bosserelle V, Azerad S, Weiss JJ, Joel ME, Aegerter P, Azouvi P; Steering Committee of the PariS-TBI study. Predictors of informal care burden 1 year after a severe traumatic brain injury: results from the PariS-TBI study. J Head Trauma Rehabil 2013; 28: 408-418.

[38] Garcia-Monzon C, Lo Iacono O, Mayoral R, Gonzalez-Rodriguez A, Miquilena-Colina ME, Lozano-Rodriguez T, Garcia-Pozo L, Vargas-Castrillon J, Casado M, Bosca L, Valverde AM and Martin-Sanz P. Hepatic insulin resistance is associated with increased apoptosis and fibrogenesis in nonalcoholic steatohepatitis and chronic hepatitis C. J Hepatol 2011; 54: 142-152.

[39] Pirhonen J, Arola J, Sadevirta S, Luukkonen P, Karppinen SM, Pihlajaniemi T, Isomaki A, Hukkanen M, Yki-Jarvinen H and Ikonen E. Continuous grading of early fibrosis in NAFLD using label-free imaging: a proof-of-concept study. PLoS One 2016; 11: e0147804.

[40] Vespasiani-Gentilucci U, Carotti S, Perrone G, Mazzarelli C, Galati G, Onetti-Muda A, Picardi A and Morini S. Hepatic toll-like receptor 4 expression is associated with portal inflammation and fibrosis in patients with NAFLD. Liver Int 2015; 35: 569-581.

[41] Jiang ZG, Tsugawa Y, Tapper EB, Lai M, Afdhal N, Robson SC and Mukamal KJ. Low-fasting triglyceride levels are associated with non-invasive markers of advanced liver fibrosis among adults in the United States. Aliment Pharmacol Ther 2015; 42: 106-116.

[42] Arrese M, Cabrera D, Kalergis AM and Feldstein AE. Innate immunity and inflammation in NAFLD/NASH. Dig Dis Sci 2016; 61: 1294-1303.

[43] Aller R, Izaola O, Ruiz-Rebollo L, Pacheco D and de Luis DA. Predictive factors of non-alcoholic steatohepatitis: relationship with metabolic syndrome. Nutr Hosp 2015; 31: 2496-2502.

[44] Zhang L, Zhang Z, Li Y, Liao S, Wu X, Chang Q and Liang B. Cholesterol induces lipoprotein lipase expression in a tree shrew (Tupaia belangeri chinensis) model of non-alcoholic fatty liver disease. Sci Rep 2015; 5: 15970.

[45] Wu KT, Kuo PL, Su SB, Chen YY, Yeh ML, Huang CI, Yang JF, Lin CI, Hsieh MH, Hsieh MY, Huang CF, Lin WY, Yu ML, Dai CY and Wang HY. Nonalcoholic fatty liver disease severity is associated with the ratios of total cholesterol and triglycerides to high-density lipoprotein cholesterol. J Clin Lipidol 2016; 10: 420-425, e421.

[46] Sookoian S, Castano GO, Scian R, Mallardi P, Fernandez Gianotti T, Burgueno AL, San Martino J and Pirola CJ. Genetic variation in transmembrane 6 superfamily member 2 and the risk of nonalcoholic fatty liver disease and histological disease severity. Hepatology 2015; 61: 515-525.

[47] Takahashi Y, Soejima Y and Fukusato T. Animal models of nonalcoholic fatty liver disease/nonalcoholic steatohepatitis. World J Gastroenterol 2012; 18: 2300-2308.

[48]   Ito M, Suzuki J, Tsujioka S, Sasaki M, Gomori A, Shirakura T, Hirose H, Ito M, Ishihara A, Iwaasa H and Kanatani A. Longitudinal analysis of murine steatohepatitis model induced by chronic exposure to high-fat diet. Hepatol Res 2007; 37: 50-57.

[49]   Van Rooyen DM, Gan LT, Yeh MM, Haigh WG, Larter CZ, Ioannou G, Teoh NC and Farrell GC. Pharmacological cholesterol lowering reverses fibrotic NASH in obese, diabetic mice with metabolic syndrome. J Hepatol 2013; 59: 144-152.

Supplementary materials & methods: western blot, immunohistochemical method

Western blot: type I collagen, type III collagen, TGF-β1, and PDGF

Hepatic cells were lysed in RIPA lysis buffer (Beyotime Biotechnology, Jiangsu, China) with 1 mM phenyl-methylsulphonyl fluoride (PMSF) (Amresco, Solon, OH, USA). After the samples were centrifuged at 10000 g for 5 minutes, protein levels in the supernatants were measured by a BCA assay kit (Beyotime Biotechnology, Jiangsu, China). For each sample, 50 μg of protein was separated on 10% polyacryl-amide electrophoresis (160 V, 2 h), and transferred to a polyvinylidenedifluoride membrane (400 mA, 2 h at 4°C). The membranes were preblocked (1 h at room temperature) with 5% skimmed milk in Tris-buffered saline-Tween-20. Subsequently, membranes were incubated overnight at 4°C with the primary antibodies: anti-Collagen I, anti-Collagen III, anti-TGFβ1, and anti-PDGF (Abcam, Cambridge, MA, USA). After wash three times, the membranes were incubated with secondary antibodies HRP-labeled goat anti-rabbit IgG (H + L) (Beyotime Biotechnology, Jiangsu, China) (1:5000) for 1 hour and followed by another three washes for preparing the visualization. Finally, the results were visualized with enhanced chemiluminescence (ECL, Millipore, Billerica, MA), and were quantitative analyzed by using a BioshineChemiQ 4600 mini chemiluminescence imaging system (Bioshine, Shanghai, China).

Immunohistochemical method: Kupffer cell, hepatic stellate cell, type I collagen, and type III collagen

After the liver sections were dewaxed in xylene and graded alcohols, the sections were hydrated and washed in phosphate-buffered saline. Afterwards, the peroxidase in the sample was inhibited by 3% H_2O_2 for 10 minutes, and then the sections were pretreated in a pressure cooker in sodium citrate buf-fer, followed by an incubation step with 5% bull serum albumin for 30 minutes to block the slides. The primary antibodies used were: anti-α-SMA (product code: ab5694, Abcam, Cambridge, MA, USA), anti-CD68 (product code: ab53444, Abcam, Cambridge, MA, USA), anti-collagen I (product code: ab34710, Abcam, Cambridge, MA, USA), and anti-collagen III (product code: ab7778, Abcam, Cambridge, MA, USA). These primary antibodies were applied overnight in a refrigerator at 4°C. After washing, a second-ary antibody, anti-rabbit mouse immunoglobulins (clone MR12/53, DakoDiagnostika, Hamburg, Germany) was added inside and incubated at 37°C for 30 minutes. Reaction products were visualized by incubation with diaminobenzidine (Liquid DAB+, DakoDiagnostika, Hamburg, Germany) and counter-stained with hematoxylin. And then, a leica microscope (Leica DM2500, Germany) was used to measure the optical density values. We scanned 10 images for each slice (10 × 2.5 original magnification; 0.22 mm^2 total area per image).

Supplementary Table 1. Nutritional differences between standard diet and high-fat, high-cholesterol diet

	Standard diet	High-fat high-cholesterol diet
Total calorific value	16.55 MJ/kg	19.19 MJ/kg
Carbohydrates	44.70%	36.40%
Crude protein	22.10%	19.30%
Fat (cholesterol)	Minor*	2.74%
Other fat	3.00%	13.26%
Crude fiber	3.30%	3.50%
Crude ash	7.80%	3.20%
Others (water, etc.)	19.10%	21.60%

*about 0.156 mg/g diet.

Supplementary Table 2. NAFLD clinical research network scoring system definitions and scores

Item		Definition 3	6	9	12	15	18	21	24
			Time (week)						

Item		Definition 3	6	9	12	15	18	21	24
Steatosis	Grade	< 33%	8	0	1	0	0	0	0	0
		33%-66%	0	8	7	6	3	0	0	0
		> 66%	0	0	0	2	5	8	8	8
	Microvesicular steatosis	Not present	8	8	2	0	1	0	0	0
		Present	0	0	6	8	7	8	8	8
Fibrosis	Stage	None	8	8	8	4	0	2	1	0
		Perisinusoidal or periportal	0	0	0	4	0	0	0	0
		Mild, zone 3, perisinusoidal	0	0	0	0	2	1	0	0
		Moderate, zone 3, perisinusoidal	0	0	0	0	5	2	2	0
		Portal/periportal	0	0	0	0	1	3	3	3
		Bridging fibrosis	0	0	0	0	0	0	1	2
		Cirrhosis	0	0	0	0	0	0	1	3
Inflammation	Lobular inflammation	No foci	8	5	7	4	1	0	1	0
		< foci per 200 × field	0	3	1	4	7	8	7	8
		> 2 foci per 200 × field	0	0	0	0	0	0	0	0
	Portal inflammation	None to minimal	8	8	3	4	2	3	5	4
		Greater than minimal	0	0	5	4	6	5	3	4
Liver cell injury	Ballooning	None	8	3	0	0	0	0	0	0
		Few balloon cells	0	5	1	0	0	0	0	0
		Many cells/prominent ballooning	0	0	7	8	8	8	8	8
Result			Steatosis	NASH without fibrosis		NASH with fibrosis		Advanced fibrosis/ cirrhosis	

(n = 8, score means the number of animals with described symptom at each time point. NAFLD: nonalcoholic fatty liver disease; NASH: nonalcoholicsteatohepatitis).

Supplementary Table 3. Biochemical characteristics of control group and model groups during the first 9 weeks HFHCD induction

	Control	3 weeks	6 weeks	9 weeks
ALT (U/L)	70.44 ± 4.03	73.80 ± 9.93	88.00 ± 15.80**	77.71 ± 21.26
AST (U/L)	164.38 ± 17.85	192.67 ± 35.42*	179.25 ± 29.26	193.86 ± 31.36*
GLU (mmol/L)	4.55 ± 0.40	6.28 ± 1.13**	6.56 ± 0.56**	7.48 ± 1.55**
TG (mmol/L)	1.11 ± 0.43	1.95 ± 0.40**	1.51 ± 0.43*	0.48 ± 0.14**
CHO (mmol/L)	2.66 ± 0.70	10.42 ± 2.47**	7.89 ± 2.89**	4.75 ± 0.87**

$*P < 0.05$, $**P < 0.01$.

Supplementary Table 4. Body weight of control group and model groups during the first 9 weeks HFHCD induction

Body weight (g)	3 weeks	6 weeks	9 weeks
Control	41.51 ± 3.71	47.89 ± 2.93	54.16 ± 5.02
Model	40.13 ± 6.20	58.93 ± 6.04**	64.64 ± 5.67**

$**P < 0.01$.